J Vet Clin 24(2) : 251-254 (2007)

Journal of Veterinary Clinics
www.ksvc.or.kr

Ovarian Papillary Adenocarcinoma in a Yorkshire Terrier Dog

Sue-Kyung Cho, Byeong-Teck Kang, Chul Park*, Jong-Hyun Yoo**, Dong-In Jung, Chae-Young Lim, Jong-Hwan Lee*, Eung-Je Woo**** and Hee-Myung Park[1]**

*Department of Veterinary Internal Medicine, *Anatomy, and **BK21 Program of Integrative Network Systems for Veterinarians in Basic Science Industrial Animals and Preventive Medicines, College of Veterinary Medicine, Konkuk University, #1 Hwayang-dong, Gwang-jin-gu, Seoul 143-701, ***Acupuncture & Meridian Science Research Center, ****College of Electronics and Information, Kyunghee University, 1 Seocheon-dong, Giheung-gu, Yongin-si,Gyeonggi-do 446-701, South Korea*

(Accepted: June 15, 2007)

Abstract : A 10-year-old intact female Yorkshire terrier dog was referred for evaluation of marked abdominal distension and hemorrhagic effusion. Abdominal radiography and ultrasonography demonstrated abdominal effusion and intraabdominal mass with anechoic cystic components. On ascites cytology, neoplastic epithelial cells with vacuolated cytoplasm and prominent nucleoli were identified. Magnetic resonance imaging (MRI) showed the well-defined, heterogeneous, and large mass filled the intraabdominal cavity. At necropsy, a large mass arising from the right ovary was observed. Histopathologically, the mass was composed of papillary structures lined by neoplastic epithelial cells. The dog was definitively diagnosed as malignant ovarian adenocarcinoma with papillary pattern based on clinical and histopathological findings.

Key words **:** magnetic resonance imaging (MRI), malignant ovarian adenocarcinoma, papillary pattern, dog.

Introduction

The ovarian tumor is uncommon in the dog with a reported incidence ranging from 0.5 to 1.2% of all canine neoplasia (1,2). There is an increased incidence of ovarian tumor in older dogs (3). The mean age of the dogs was greater than 10 years. However granulosa cell tumor (GCT) and teratoma occur at a slightly younger age than the other ovarian tumors (2,7). Boxers, German shepherds, Yorkshire terriers, Poodles, Boston terriers, and mixed breed dogs were the most commonly affected breeds (6,7).

Canine ovarian tumors can be divided into three major categories: (a) germ cell, (b) epithelial cell, and (c) sex cord stromal tumors. Among them epithelial cell tumors are most common and include papillary adenomas/cystadenomas, papillary adenocarcinomas (PAC), rete adenomas, and undifferentiated carcinomas (1,6). The PAC was characterized by a large size and involvement of the ovarian stroma, bursa, and the peritoneum (8).

Previously, two cases of ovarian adenocarcinoma were reported in Korea (5). This case report firstly describes magnetic resonance imaging (MRI) features as well as clinical and histopathologic findings of malignant ovarian adenocarcinoma with papillary pattern in a dog.

[1]Corresponding author.
E-mail : parkhee@konkuk.ac.kr

S. K. Cho and B. T. Kang contributed equally to this work as the co-first authors

Case

A 10-year-old intact female Yorkshire terrier was referred for evaluation of marked abdominal distension and hemorrhagic effusion. Abdominal distension had been gradually progressed during one month. Polyuria (PU) and polydipsia (PD) were concurrently observed by owner. The hemorrhagic abdominal effusion was firstly shown in local hospital two days before the presentation.

Physical examination revealed that abdominal distension, hyperthermia (39.38°C), tachypnea, and tachycardia (240 beats per minute). On complete blood count (CBC), mild leukocytosis ($27.40 \times 10^3/\mu L$, reference range; $6.0\text{-}17.0 \times 10^3/\mu L$) and mild anemia (35.8%, reference range; 37.0%-55.0%) were found. The serum chemistry profiles revealed mild hypoalbuminemia (2.4 g/dL, reference range; 2.6-4.0 g/dL) and severely elevated γ-Glutamyltransferase (GGT) (319 mg/dL, reference range; 5-14 mg/dL). Typical radiographic finding showed uniformly distributed homogenous soft tissue density throughout the distended abdomen. Diffuse decrease of serosal detail suggested peritoneal effusion. Additionally, craniolateral displacement of gas trapped intestine was detected on ventrodorsal view (Fig. 1). On abdominal ultrasonography, solid mass with multiple cystic components (Fig. 2) and free abdominal fluid throughout the distended abdomen were observed. Serosanguineous colored ascites was obtained by abdominal paracentesis. Specific gravity was 1.025 and total protein concentration was 2.6 g/dL. On cytologic examination of the specimens, neoplastic epithelial cells with moderate to marked cellularity were seen. Indi-

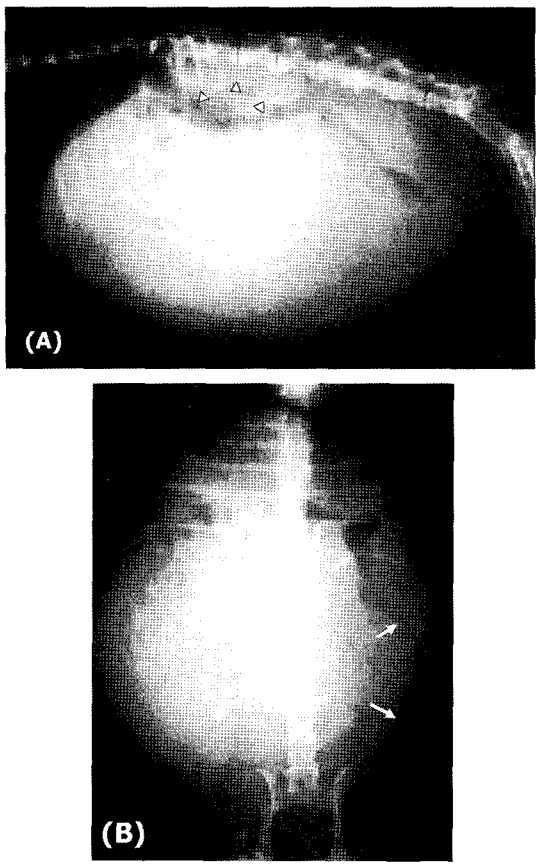

Fig 1. Lateral (A) and ventrodorsal view (B) of the abdominal radiography. Uniformly distributed homogenous soft tissue density is observed throughout the distended abdomen. The craniolateral displacement of gas-trapped intestine (arrows) and dorsal shift of left kidney (arrow heads) are shown.

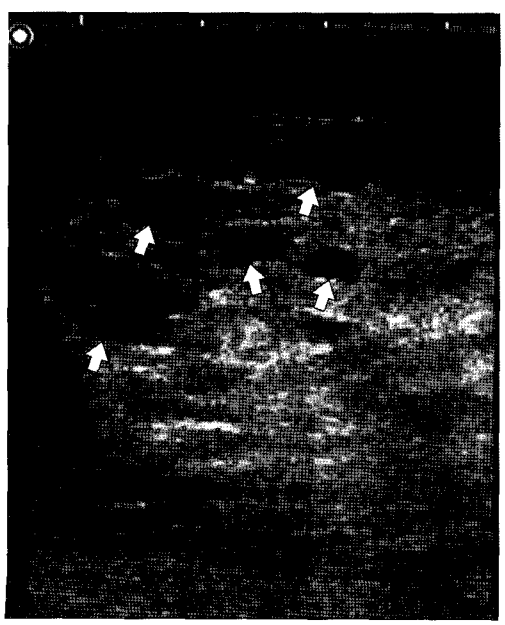

Fig 2. Sagittal ultrasonographic image of the abdominal mass. Note the presence of multiple anechoic lesions (arrows) in a solid mass.

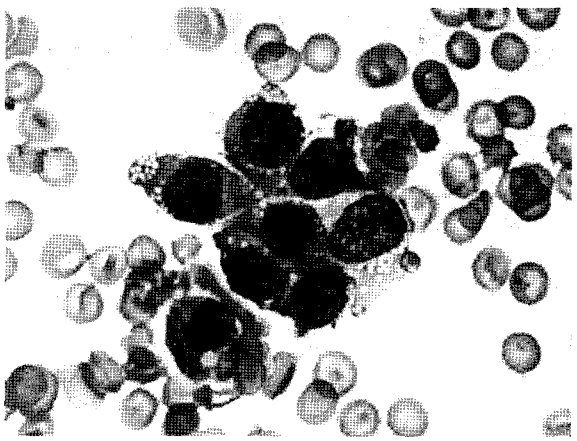

Fig 3. Cytologic preparation of acites. A cluster of pleomorphic epithelial cells with a single round to oval nucleus, multiple prominent nucleoli, and vacuolated cytoplasm were seen (Diff Quick, X 1,000).

vidual cells appeared to be pleomorphic and had a single round to oval nucleus, multiple prominent nucleoli, and vacuolated cytoplasm. Anisocytosis and anisokaryosis were also noted (Fig. 3). Thus effusions were classified as modified transudate.

Through above-mentioned checkup, we suspected that the tumor might be originated from ovary or uterus and metastasized to other regions. Thus we executed excretory urography (EU) to validate metastasis to the kidney because the kidney is most common organ invaded by the tumor of reproductive system. However the results were not remarkable except dorsal displacement of bilateral kidneys.

One day after the presentation, we performed MRI scanning to identify the origin of tumor and metastasis to other organs. MRI of the abdomen was obtained using a 0.2 Tesla magnet (E-Scan®, ESAOTE, Italy) in transverse, sagittal, and dorsal T1- and T2- weighted images (WI). A heterogeneous huge mass, which entirely filled abdomen, was observed (Fig. 4). On T1-WI, hypointensity lesions were found throughout the mass, especially in the central portion (Fig. 4A). Two round hypointensity lesions, which surrounded by isointensity rim, were identified at the front and the opposite site of left ovary (Fig. 4A, C, and E). At the same places, hyperintensity lesions were found on T2-WI (Fig. 4B, D, and F). These were suspected to cystic changes of the mass. The caudal portion of the mass closely adjoined the left ovary (Fig. 4C-F). The left ovary was mildly enlarged, and had T1 hypointensity and T2 hyperintensity lesions (Fig. 4C and D). Based on these findings, it was suspected that the mass was originated from the right ovary and affected the left ovary. The dog died at 8 hours after scanning due to severe respiratory distress.

At necropsy, the mass originated from the right ovary and metastasized to the left ovary. Large-sized mass (13 cm × 16 cm × 10 cm) was well-encapsulated and adhered to mesentery (Fig. 5). Dorsal part of the mass was ruptured and necrotic materials flowed out. Nodular lesions were found in liver parenchyma. Histopathologically, the mass and the left ovary

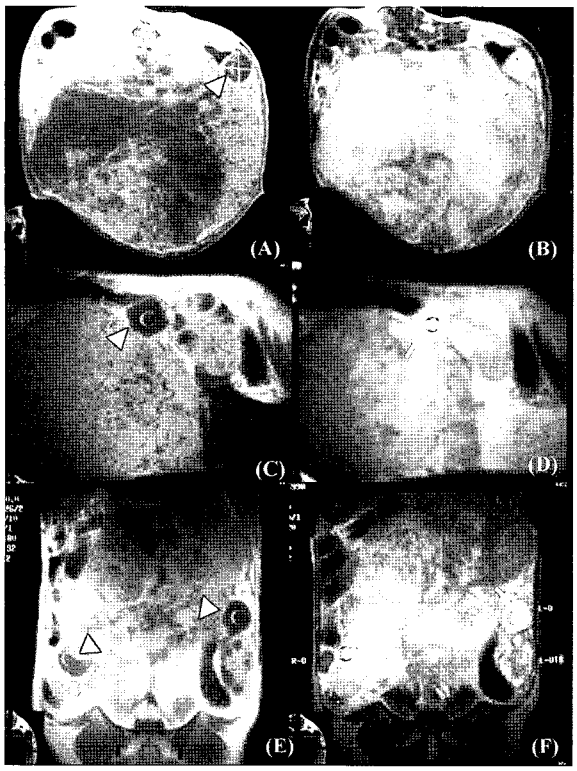

Fig 4. MR images of the abdomen. (A) and (B): transverse view; (C) and (D); sagittal view; (E) and (F); dorsal view. A heterogeneous large mass was observed. On T1-weighted images (WI), hypointensity lesions were found throughout the mass, especially in the central portion (A). Two round hypointensity lesions (arrow heads) were identified at the front and the opposite site of left ovary (A, C, and E). At the same places, hyperintensity lesions (arrows) were found on T2-WI (B, D, and F). The caudal portion of mass closely adjoined the left ovary (C-F). The left ovary was mildly enlarged, and had T1 hypointensity (C) and T2 hyperintensity lesions (D). C: cyst; M: mass; LO: left ovary; RO: right ovary.

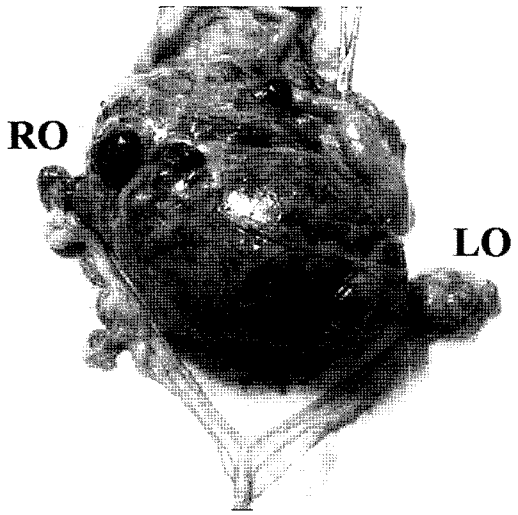

Fig 5. Large-sized mass (13 cm × 16 cm × 10 cm) originated from the right ovary was well-encapsulated and adhered to mesentery. LO: left ovary; RO: right ovary.

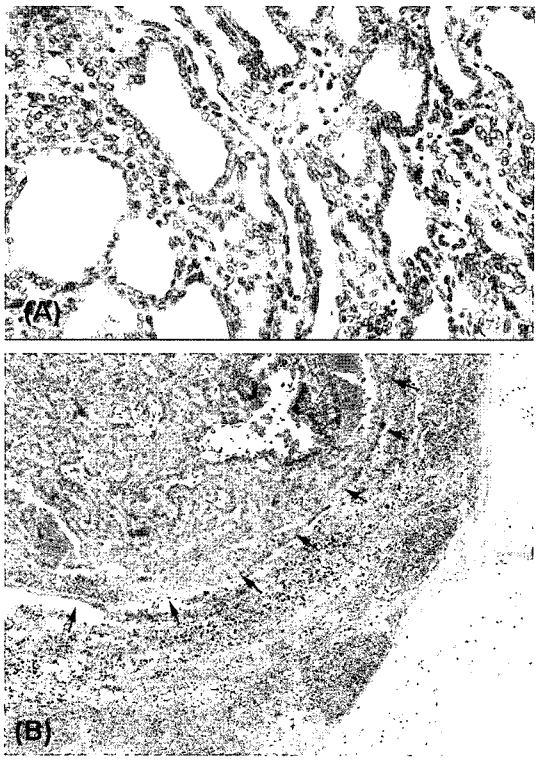

Fig 6. (A) The ovarian mass was composed of papillary structures lined by single or occasionally multiple layers of the neoplastic cuboidal cells (H&E, X 400). (B) The adjacent lymph node: note the metastatic carcinoma (arrows) within a lymph node (H&E, X 40).

were composed of papillary structures lined by neoplastic epithelial cells (Fig. 6A). Malignant glandular epithelium of the ovary was multiplicated and metastasized to the adjacent lymph node (Fig. 6B). Thus the dog was definitively diagnosed as an ovarian PAC.

Discussion

The apparent low incidence of canine ovarian tumors is influenced by the source of the material, as it depends upon the number of bitches that are neutered at an early age (2). In this case, the dog was 10-year-old that was well known to median ages of the primary ovarian tumor (6). Moreover, Yorkshire terrier dog was known to the one of the most commonly affected breeds (7).

The clinical signs of the dogs affected primary ovarian tumors are below; (a) presence of an intraabdominal mass with or without ascites (palpable mass and abdominal distention); (b) hormone disturbances and uterine abnormalities (vulvovaginal discharge, abnormal estrus behaviour, and PU/PD); and (c) metastatic spread (dyspnea and systemic signs) (2). Similarly, our patient had most of these clinical signs. The dog had a palpable mass and ascites throughout the distended abdomen. Also PU/PD and systemic signs such as tachypnea, tachycardia, and hyperthermia were shown. However uterine abnor-

malities, such as pyometra or cystic endometrial hyperplasia, were not detected on ultrasonography and necropsy. According to one study of 71 canine ovarian tumor cases, the rate of epithelial tumor affects uterus was relatively low (6).

In this case, mild leukocytosis and anemia were noted. However these are not considered specific findings to diagnosis ovarian tumor (2,8). Severe elevation of GGT may be resulted from the focal lesion of the liver caused significant cholestasis. The accumulation of body-cavity fluids could result in decreased serum albumin and globulin concentrations (panhypoproteinemia). Malignant effusions may be developed by edema within the ovarian tumor, which cause leakage of fluid throughout the tumor capsule and secretions from metastatic peritoneal implants (4). Cytology of the effusions showed that the possibility of epithelial cell tumor and malignancy. Furthermore, various imaging techniques were used for the diagnosis of ovarian tumor and the detection of metastasis. Radiography made the speculation of presence of intraabdominal mass and the nature of the mass was identified through the ultrasonography. EU and MRI helped the identification of the tumor origin.

Generally, surgical removal (ovariohysterectomy) is the recommended in the majority of canine ovarian tumors (2). In this case, ovariohysterectomy was not performed because of lack of the knowledge about metastasis and origin as well as large size of the tumor. Ultrasonography is a reliable technique to determine the origin of a mass. However, if the masses are unilateral and measured over 10 cm in diameter, it is difficult to ascertain that they had an ovarian origin, as other neoplasms can grow to reach the area caudal to the kidneys (2). In this case, the diameter of mass was over 10 cm. Thus MRI scanning was performed to know the features of mass exactly before surgical treatment.

This case report describes clinical, MRI, and histopathological features of a malignant ovarian PAC occurred in the dog. Especially, cytologic examination of ascites and advanced imaging techniques were useful for the diagnosis and the judgement of prognosis in the abdominal neoplasm.

Acknowledgment

This work was supported by the SRC/ERC program of MOST/KOSEF (R11-2002-103).

References

1. Bertazzolo W, Dell' Orco M, Bonfanti U, DeLorenzi D, Masserdotti C, De Marco B, Caniatti M, Roccabianca P. Cytologic features of canine ovarian tumours: a retrospective study of 19 cases. J Small Anim Pract 2004; 45: 539-545.
2. Diez-Bru N, Garcia-Real I, Martinez EM, Rollan E, Mayenco A, Llorens P. Ultrasonographic appearance of ovarian tumors in 10 dogs. Vet Radiol Ultrasound 1998; 39: 226-233.
3. Goodwin JK, Hager D, Phillips L, Lyman R. Bilateral ovarian adenocarcinoma in a dog: ultrasonographic-aided diagnosis. Vet Radiol 1990; 31: 265-267.
4. Hayes A, Harvey HJ. Treatment of metastatic granulosa cell tumor in a dog. J Am Vet Med Assoc 1979; 174: 1304-1306.
5. Jeong SM, Lee CH, Kim WH, Yang JH, Kim DY, Choi MC, Yoon JH, Lee JM, Kweon OK, Nam TC. Ovarian cancers in 2 dogs. J Vet Clin 2001; 18: 438-441.
6. Patnaik AK, Greenlee PG. Canine ovarian neoplasm: a clinicopathologic study of 71 cases, including histology of 12 granulosa cell tumors. Vet Pathol 1987; 24: 509-514.
7. Sforna M, Brachelente C, Lepri E, Mechelli L. Canine ovarian tumours: a retrospective study of 49 cases. Vet Res Commun 2003; 27: 359-361.
8. Yotov S, Simeonov R, Dimitrov F, Vassilev N, Dimitrov M, Georgiev P. Papillary ovarian cystadenocarcinoma in a dog. J S Afr Vet Assoc 2005; 76: 43-45.

요크셔테리어에서 발생한 난소 유두모양샘암종

조수경 · 강병택 · 박철* · 유종현** · 정동인 · 임채영 · 이종환* · 우응제**** · 박희명**[1]**

건국대학교 수의과대학 내과학 교실, *해부학 교실, **BK21 수의기초 · 산업동물 · 예방의학 통합네트워크 연구인력양성 사업단, ***경희대학교 침구경락과학연구센터, ****경희대학교 전자정보대학 동서의료공학과

요 약 : 10년령의 중성화되지 않은 암컷 요크셔테리어가 심한 복부확장과 출혈성 삼출물에 대한 평가를 위해 내원하였다. 복부 방사선과 초음파 검사상에서 삼출물과 무에코의 낭성 구성물 들을 지닌 복강 내 종괴가 확인되었다. 복수의 세포검사에서 공포화된 세포질을 지닌 종양성 외피 세포들과 현저한 핵들이 관찰되었다. 자기공명영상에서는 잘 분획되고, 이질성의 큰 종괴가 복강 내를 채우고 있었다. 부검 상에서는 우측 난소로부터 유래한 큰 종괴가 관찰되었다. 조직병리학적 검사에서는 종양성 외피세포들로 이루어진 유두모양 구조들로 종괴가 구성되어있는 것을 확인 할 수 있었다. 환견은 임상 및 조직병리학적 소견들에 근거하여 유두모양의 악성 난소 샘암종으로 최종 진단되었다.

주요어 : 자기공명영상, 악성 난소 샘암종, 유두모양, 개